

First-principles study of the atomic reconstructions and energies of Ga- and As-stabilized GaAs(100) surfaces

Guo-Xin Qian

Department of Physics, Brookhaven National Laboratory, Upton, New York 11973-5000

Richard M. Martin

Department of Physics, University of Illinois at Urbana-Champaign, Urbana, Illinois 61801

D. J. Chadi

Xerox Corporation, Palo Alto Research Center, Palo Alto, California 94304

(Received 18 November 1987; revised manuscript received 23 May 1988)

We have carried out *ab initio* total-energy density-functional calculations to study the reconstructions of GaAs(100) surfaces as a function of Ga and As surface coverage. Equilibrium atomic geometries and energies for Ga- and As-stabilized 1×1 , 2×1 , 1×2 , and 2×2 surfaces consisting of various combinations of dimers and vacancies were determined. Dimerization of Ga (As) surface atoms is calculated to lower the energy by 1.7 eV (0.7 eV) per dimer and to lead to the most stable atomic configurations. For half-monolayer coverages, relaxation energies are very large, and *nondimerized* structures are only slightly (0.03–0.05 eV per 1×1 cell) higher in energy. Asymmetric dimers were tested for As surfaces and found to be higher in energy than symmetric dimers. The stability of surfaces in equilibrium with Ga and As sources is considered and it is shown that the chemical potentials are restricted within limits set by the free energies of the elemental *bulk* phases of Ga and As. *Ab initio* calculations of these bulk energies at $T=0$ K determine the limiting chemical potentials and also the heat of formation, which we find to be 0.73 eV per GaAs pair, compared with the experimental value of 0.74 eV. Our calculations indicate that with excess bulk As available, a full monolayer coverage of As is energetically more favorable than a half-monolayer coverage, whereas with excess Ga available, the surface energy of full and half-monolayer coverages are nearly the same. To examine the effects of larger unit-cell dimensions on total energies, we rely on results from tight-binding calculations. For half-monolayer coverages, 2×4 unit cells are found to have a significantly lower energy than 2×2 cells not because of a greater lattice relaxation but because of orbital rehybridization effects which are not possible in a smaller cell. The results of the *ab initio* and tight-binding calculations indicate that the optimal surface coverage for Ga- and As-terminated surfaces is less than a full monolayer.

I. INTRODUCTION

The (100) surface of GaAs exhibits a rich variety of structures, often with large unit cells, as a function of surface stoichiometry and temperature.^{1–3} There has been much interest in understanding the microscopic nature of these reconstructions but very little is known with certainty at present regarding the surface atomic structure.^{4,5} Since the (100) surface is polar, a theoretical determination of its atomic structure requires calculations of minimum energy geometries as a function of Ga and As coverage, or equivalently as a function of Ga and As chemical potentials.

The present paper is aimed at a systematic study of the GaAs(100) surface as a function of Ga and As chemical potentials using a first-principles pseudopotential and local-density-functional formalism. We examine both Ga- and As-terminated surfaces with surface coverages of $\Theta=\frac{1}{2}$ and $\Theta=1$. For half-monolayer situations, two atomic configurations are examined: 1×2 -Ga (and 2×1 -As) vacancy models, and 2×2 vacancy plus dimer models in which the remaining surface atoms form di-

mers. For the $\Theta=1$ case, we also consider two atomic configurations: 2×1 -Ga (and 1×2 -As) dimer models and 1×1 relaxed surfaces. The total energies of these systems are calculated in an energy-minimization procedure which gives the optimal atomic relaxation geometries. For $\Theta=\frac{1}{2}$ cases, the surface energies are determined from the increase in total energy above that of bulk GaAs with the *same* number of Ga and As atoms and are compared with our previous theoretical results for the cleavage energy of the (110) surface.⁶ Tight-binding calculations are used for examining the effects of larger 2×4 unit cells on the total-energy and atomic structure. The effects are found to be large, especially for the half-monolayer coverage case.

An important part of this work is establishing the appropriate chemical potentials which are needed for the determination of the stability of the surfaces in equilibrium with elemental Ga and As in either gaseous or condensed phases. We show that the allowable ranges of the potentials under equilibrium conditions are fixed by the elemental bulk phases, and we carry out *ab initio* calculations of the energies of bulk Ga and As at $T=0$ K. As a

test of these calculations, we compute the heat of formation of GaAs and find it to be in exceptionally good agreement with experiment. Using the calculated limits for the chemical potentials, we predict stable surfaces for the allowed intermediate values of the potentials.

The present work is similar in many ways to that of Kaxiras *et al.*,⁷ who carried out density-functional calculations for (111) and $(\bar{1}\bar{1}\bar{1})$ GaAs surface with different stoichiometries. Both calculations emphasize the role of the chemical potentials of Ga and As in determining the surface stoichiometry. In this work we show that it is possible to set stricter limits on the allowable ranges of the chemical potentials and, therefore, to set more definitive limits on the surface stoichiometry and structure. For the (100) surface we find a number of structures with similar energies, leading to the possibility of more complex reconstructions on this surface than on (111) or $(\bar{1}\bar{1}\bar{1})$.

The paper is organized as follows. Section II describes first-principles, self-consistent density-functional calculations, with out newly generated soft-core pseudopotentials. The various test results for GaAs bulk as well as Si(111)- 2×1 , Si(111):As, and GaAs(110) surfaces from this pseudopotential are also presented and discussed. Section III is devoted to the discussion of the thermodynamics of GaAs surfaces and the calculations of the total energies of bulk GaAs, Ga, and As. Section IV presents the results of our total-energy calculations for different reconstructions of Ga- and As-terminated GaAs(100) surfaces. The consequences of these results for the stoichiometries and reconstructions of GaAs(100) surfaces are analyzed in Sec. V, where tight-binding and *ab initio* results are used in conjunction with each other to examine the effects of 2×4 reconstructions on surface energies and composition. A brief summary of the work is presented in Sec. VI.

II. METHOD OF CALCULATION AND TEST RESULTS FOR SOFT-CORE PSEUDOPOTENTIALS

A. Method

Our total-energy calculation is based on the self-consistent local-density-functional approach of Hohenberg, Kohn, and Sham,⁸ which we apply in the momentum-space formalism as summarized in Ref. 9. Previous applications of the method to surfaces have been presented in Refs. 5, 6, and 10. The Ceperley-Alder form¹¹ of exchange-correlation energy was used throughout the work. Here we use the norm-conserving, nonlocal atomic pseudopotentials of Ga and As which were generated according to the Kerker scheme,¹² which is described below.

We would like to say a few words about pseudopotential calculations for systems with large unit cells. It is very well known that pseudopotentials are *not* unique, and there are many potentials which give a good description of atomic eigenvalues and eigenfunctions. Accurate nonlocal pseudopotentials are generally *hard*; i.e., they are strongly varying for small distances close to the ion cores. We have tested the original recipe of Kerker, as well as the pseudopotentials given by Bachelet *et al.*,¹³

and find that typically a 12–18-Ry energy cutoff in the plane-wave basis expansion is needed in order to achieve good convergence. While many total-energy calculations for bulk systems have been done using a cutoff of 12 Ry or larger for surface systems that have a larger number of atoms in the unit cell it has been feasible so far to consider only about a 6-Ry energy cutoff in the plane-wave expansion.^{5–7,10,14,15}

Instead of doing a surface calculation with a 6-Ry cutoff for the hard-core pseudopotential, we generated softer pseudopotentials which are better converged at a 6-Ry cutoff. The softer pseudopotentials were generated by the following method. In the Kerker approach,¹² the nodeless pseudovalence wave function is taken to be identical to the real wave function outside the chosen “core” radius r_c , and the inner part is represented by a smooth analytical function which joins the atomic wave function at r_c . Kerker required r_c to be inside the outmost maximum of the atomic wave function, with its value chosen to minimize the kinks. However, if this core radius is chosen to be *larger*, the pseudopotential generated from the pseudovalence wave function is *softer*. In the present work r_c is chosen to be larger than the outermost maximum of the appropriate *s*, *p*, and *d* atomic wave functions. Our (Kerker’s) values in atomic units for the r_c ’s in Ga are $r_s=2.76$ (1.68), $r_p=3.37$ (1.95), $r_d=5.85$ (3.21). The corresponding values for As are $r_s=2.35$ (1.50), $r_p=2.87$ (1.65), $r_d=4.50$ (2.59). The softer pseudopotentials are still norm-conserving so that the total charge is still conserved at r_c , and the electrostatic potential is correct outside the core radius. The accuracy increases as the bond-length becomes larger than $r_c^{\text{Ga}}+r_c^{\text{As}}$. Since the softer potentials are in general less accurate than harder ones, it is necessary to carry out tests to ensure that they give a satisfactory description of bulk properties. Some test results of hard-core and soft-core pseudopotential are described in Sec. II B.

Our calculations for the GaAs(100) surfaces are performed with a basis set consisting of plane waves with an energy cutoff of 6 Ry (~ 565 plane waves for the 2×1 and ~ 1130 plane waves for a 2×2 periodicity). Eight (four) special sampling points in the surface primitive Brillouin zone are used for the 2×1 (2×2) periodicities in the energy summation. For each surface reconstruction, we start from the “best guess” geometry, or ideal geometry. Self-consistent pseudopotential calculations are carried out until the electron charge density is self-consistent. At the same time, the quantum-mechanical forces on the atoms are calculated using the Hellmann-Feynman theorem⁹ and the atoms are moved so as to minimize the total energy. This procedure is repeated until the forces become negligible and the optimal atomic configurations as well as minimum total energies are obtained.

B. Tests of soft-core versus hard-core pseudopotentials for GaAs

Figure 1(a) shows the electronic band structure of bulk GaAs along some symmetry lines, calculated from pseudopotentials generated from the original Kerker approach, with energy cutoffs at 6 (dashed lines) and 12 Ry

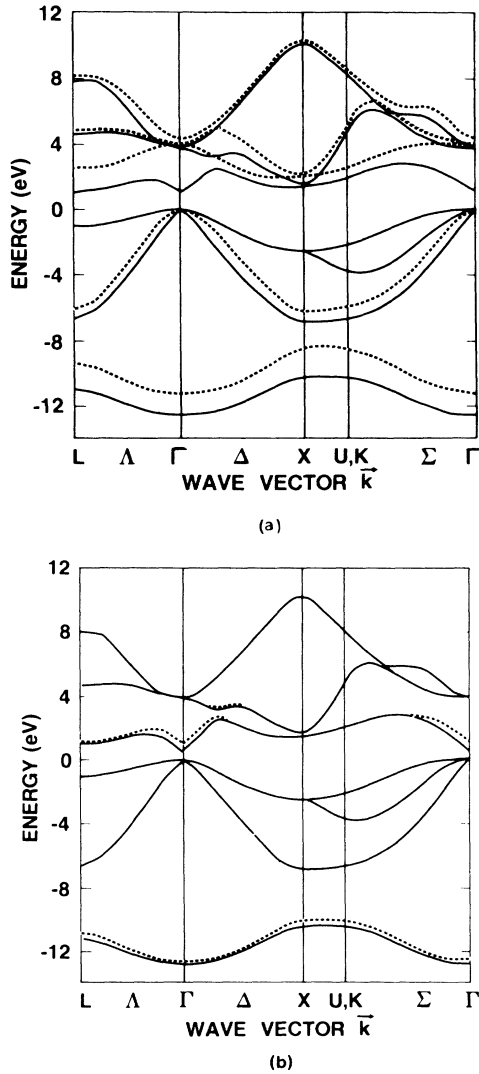


FIG. 1. Electronic energy band structure of bulk GaAs along some high symmetric lines for pseudopotentials generated from Kerker scheme, with an energy cutoff of 12 Ry (solid lines); 6 Ry (dashed lines). Part (a) is for hard potentials and (b) for soft potentials as described in the text.

(solid lines), in the plane-wave basis expansion. We see that a 6-Ry cutoff (corresponding to ~ 77 plane waves) is *not* sufficient in describing the bulk electronic properties. For example, the lowest conduction band shifts by $\sim 1-3$ eV and the order of bands changes at Γ . However, the results for the 12-Ry energy cutoff (corresponding to ~ 222 plane waves) are better converged. If the energy cutoff is increased to 18 Ry, the major change is in the first conduction band at Γ and it lowers the band gap from 1.0 to 0.4 eV.

Figure 1(b) is the band structure of bulk GaAs along the same symmetry lines, calculated from our soft pseudopotentials. Solid lines and dashed lines represent 12- and 6-Ry energy cutoffs. We can see that convergence has been reached fairly well for the 6-Ry cutoff. We also compared the band structure of bulk GaAs along the same symmetry lines calculated from hard pseudo-

tentials and from our soft pseudopotentials for a large energy cutoff (18 Ry). The agreement between the two is within the width of the lines in the figures.

As further tests of the pseudopotential, we calculated the total energy and other ground state properties of bulk GaAs. A comparison of the calculated equilibrium bulk lattice constant can be found in Table I. The lattice constant found with the hard potential, 5.55 Å, agrees well with previous work¹⁶ on GaAs which found 5.57 Å using a different form of the exchange-correlation energy. However, we see that there is a much larger change of the calculated lattice constant as a function of energy cutoff for the harder potential than for softer one. In the surface calculations below we have fixed the lattice constant in the x - y plane parallel to the surface to be the theoretical equilibrium value corresponding to a cubic lattice constant of 5.52 Å which is 2% smaller than the experimental measured value of 5.65 Å. This is essential if we want the central part of the slab to be in equilibrium with a locally cubic structure. If we had chosen a different lattice constant, e.g., the experimental value, the forces would not be zero in the "bulk" region. As another test, we calculated the phonon frequency using both a hard potential and our soft potential, at a relatively high-energy cutoff (18 Ry) in the plane-wave expansions. The difference was found to be only 2.5%.

Another independent test of bulk properties for both types of pseudopotentials is the heat of formation of bulk GaAs from bulk Ga and bulk As. We will discuss the calculations of total energies of bulk Ga and bulk As in more detail in the following section. The results given there show that the hard pseudopotential gives excellent results with a relatively high-energy cutoff (12 Ry or more), but the calculated heat of formation is off by about 1 eV if the energy cutoff is reduced to 6 Ry. A similar calculation with soft pseudopotentials is converged at a 6-Ry energy cutoff. Although there is some error (~ 0.4 eV) due to the soft potential, this can be corrected as we show in Sec. III. We conclude that, since we are limited to a small energy cutoff (~ 6 Ry) in the plane-wave expansion for our surface calculation, then the use of soft pseudopotentials is more appropriate than hard pseudopotentials.

C. Test results for Si(111)- 2×1 , Si(111):As, and GaAs(110) surfaces

We have carried out the following three test calculations for other surface systems with our soft pseudopotentials at an energy cutoff of 6 Ry.

(1) *Si(111)- 2×1 cleaved surface.* The surface energy for the π -bonded chain model was calculated using four

TABLE I. The lattice constant of bulk GaAs calculated from both hard and soft pseudopotentials at 6- and 12-Ry energy cutoff, compared with the experimentally measured value of 5.65 Å.

	6 Ry	12 Ry
Hard pseudopotential	5.42 Å	5.55 Å
Soft pseudopotential	5.48 Å	5.52 Å

special sampling points in the surface primitive Brillouin zone. The surface energy was found to be 0.33 eV per surface atom lower than that of the ideal Si(111) surface, in good agreement with the value of 0.36 eV, which was also calculated using a nonlocal pseudopotential.¹⁵

(2) *Si(111):As*. This is an ideal 1×1 surface with As atoms sitting at the topmost silicon layer, which has been studied experimentally and theoretically.¹⁷ Self-consistent total energy and force calculations were carried out for three geometries: As atoms exactly on the ideal silicon positions, and As atoms displaced towards the vacuum by 0.13 and 0.19 Å. Since our calculated forces on As at 0.13 Å (0.19 Å) are 50% (15%) of the forces at the ideal sites, we estimate that the equilibrium position for As atoms is ~ 0.22 Å away from ideal Si sites. This is in general agreement with the previous calculation,¹⁷ where the equilibrium positions for As were found to be 0.19 Å away from ideal Si sites. We believe that the discrepancy between 0.19 and 0.22 Å is within the range of the numerical uncertainties of the calculations.

(3) *GaAs(110) buckled surface*. This is a well-studied surface, both experimentally and theoretically. The results of our calculations are reported in a separate paper.⁶ To summarize, the surface atomic configuration is in general agreement with previous theoretical work and with low-energy electron diffraction (LEED) measurements.¹⁸ In addition, the surface cleavage energy is calculated to be 1.22 eV per surface unit cell, in excellent agreement with the experimentally measured value¹⁹ of 1.21 eV per surface unit cell. The photoelectric threshold (or ionization potential) is calculated to be 4.94 eV, which compares well with the experimentally measured values²⁰ of 5.15–5.75 eV. The test calculations for the GaAs(110) surface and the good agreement with experimental data are of significance to the present work because both calculations employ the same soft-core pseudopotentials and the same energy cutoff (6 Ry).

III. THERMODYNAMICS OF GaAs SURFACES AND THE TOTAL ENERGIES OF BULK GaAs, Ga, AND As

Since the goal of our present work is to predict the stability of GaAs(100) surfaces under realistic experimental conditions, we must consider the nature of the experiments in order to decide which quantities should be determined from the *ab initio* calculations. So long as the surface is in equilibrium with its surroundings, the stability may be determined following standard thermodynamics²¹ from the free energy and the chemical potentials μ_i of each type of atom i . The chemical potentials take into account the fact that the numbers of atoms are conserved in reactions at the surface, so that changes in the total free energy of the system when a Ga or As atom is interchanged between the surface and a reservoir can be determined. By incorporating the appropriate chemical potentials, we can take into account different experimental conditions and predict the stability of different surface structures. This approach is clearly appropriate when the surface is in equilibrium with the bulk and other relevant reservoirs. An example is a recent work which

reported phase transitions on the (100) surface of InAs as a function of As over-pressure and temperature.²² We may note that there may be other cases in which the reactions are not in equilibrium and may be governed by rate limiting kinetic factors. Such situations are beyond the scope of the present work and will not be considered here. We will be content if we can successfully use *ab initio* methods to make meaningful predictions for the equilibrium case.

In this section we address two issues: (i) the nature of the free energies of the different phases, the definition of the chemical potentials, and general conclusions on the allowable ranges of the chemical potentials for which the surface can be in equilibrium; and (ii) the choice of the best “standard” states for the elements Ga and As, and the compound GaAs, for which the theoretical results will be most meaningful.

A. Chemical potentials for Ga and As

The chemical potential μ_i is defined to be the derivative of the Gibbs free energy $G = E + PV - TS$ for a given phase with respect to the number of particles of type i : $\mu_i = dG/dn_i$.²¹ Since in equilibrium the chemical potential μ_i of a given atomic species is the same in all its phases which are in contact, each μ_i can be considered as the free energy per particle in each reservoir for particle i . For condensed states (e.g., the GaAs surfaces, bulk GaAs, or bulk Ga or As), the Gibbs free energy is the total energy at zero temperature plus a negative-definite temperature-dependent term which involves a simple integral of the specific heat.²¹ The PV term is completely negligible for pressures considered here. Although the temperature-dependent term can be included in principle, we ignore it in the present work for the following reasons. First, it is not feasible to calculate the entropies of the various bulk and surface states. Second, the temperature-dependent terms tend to cancel for the relevant *differences* between the free energies of condensed states so that their contributions are small. Third, this approximation has been implicit in all of the recent (rather successful) density-functional work calculating phase transitions using only the energy at $T=0$. Thus, for *condensed phases*, we ignore the temperature dependence and set the chemical potential μ equal to the total energy E per atom calculated at $T=0$.

For gaseous phases, on the other hand, the effect of T and P upon the chemical potential cannot be ignored. As is well known in gas theory,²¹ μ depends logarithmically upon T and P and the large variations in μ can be used to control the state of the condensed phases in equilibrium with the gas. In general, the function $\mu_i(P, T)$ is complicated but can in principle be determined experimentally for any gas. Nevertheless, even without a detailed knowledge of the chemical potentials as a function of P and T , we can establish ranges for $\mu_i(P, T)$ which are relevant for the determination of the surface structures under equilibrium conditions. Although the gas expressions alone permit any value of the μ_i , there are limits on the allowable range in equilibrium with all possible phases. In particular, the chemical potential for each ele-

ment cannot be above that of the bulk elemental phase. It may equal the bulk chemical potential (in which case there is in general bulk material present and the surface is in equilibrium with the elemental condensed bulk phase) or it may be below the bulk chemical potential (in which case the bulk is not stable and the surface is in equilibrium with a gaseous phase).

In addition, the bulk solid GaAs is a reservoir which can exchange atoms with the surface. If the surface is in equilibrium with the bulk, pairs of Ga and As atoms can be exchanged with the bulk, for which the energy is the total bulk energy per pair. This requires that the sum of the μ_i for Ga and As equal the bulk energy per pair. It is useful to note that the bulk energy may be equated to the sum of the energies of bulk Ga and bulk As minus the heat of formation ΔH_f , which is 0.74 eV per pair.²³ (Note that this requirement on the sum of the chemical potentials is modified if one accounts for the fact that the bulk can exchange unpaired Ga or As atoms by creating defects. This effect may be large at very elevated temperatures but is not relevant under usual growth conditions and temperatures where the small number of bulk defects do not cause gross changes in the surface stoichiometry.) Thus equilibrium with the bulk leads to the relation

$$\begin{aligned}\mu_{\text{Ga}} + \mu_{\text{As}} &= \mu_{\text{GaAs(bulk)}} \\ &= \mu_{\text{Ga(bulk)}} + \mu_{\text{As(bulk)}} - \Delta H_f.\end{aligned}\quad (1a)$$

Finally, making use of the above limits on the individual μ_i set by the bulk elements, one finds that the surface can be in equilibrium with its surroundings *only* if the chemical potentials are within both upper and lower limits:

$$\mu_{\text{As(bulk)}} - \Delta H_f \leq \mu_{\text{As}} \leq \mu_{\text{As(bulk)}}, \quad (1b)$$

$$\mu_{\text{Ga(bulk)}} - \Delta H_f \leq \mu_{\text{Ga}} \leq \mu_{\text{Ga(bulk)}}. \quad (1c)$$

Thus each μ is restricted to be in a 0.74-eV range below its respective bulk value.

The equilibrium state of the surface as a function of composition is determined by minimizing the function²¹

$$G_{\text{surface}}(n_i) - \sum_i \mu_i n_i \approx E_{\text{surface}}(n_i) - \sum_i \mu_i n_i. \quad (2)$$

Here $G_{\text{surface}}(n_i)$ is the surface free energy as a function of the variable composition and the approximate equality above amounts to replacing G by the total surface energy $E(n_i)$ at $T=0$. We will analyze our results below taking the μ_i for the extreme limiting cases of equilibrium with bulk Ga and bulk As. In Sec. V we show how all other cases can be found by a simple modification of the chemical potentials.

It may be noted that the above analysis of the chemical potential is quite different from that of Kaxiras and co-workers in a recent series of papers.⁷ These authors carried out calculations comparable to ours for the (111) and $(\bar{1}\bar{1}\bar{1})$ surfaces of GaAs. They also introduce chemical potentials, but assumed that the appropriate potential for As was that of As_2 molecules at zero temperature, i.e., the total energy of As_2 . Since the energy of the molecule is *higher* than the energy of bulk As by 1.15 eV per atom,²³ this is equivalent to choosing the chemical potential μ_{As}

far above the value for which bulk As forms, i.e., far outside the allowable range for equilibrium. It is our position that the use of the binding energy in place of the free energy for the gas is incorrect. There are three clear reasons for our conclusion: (i) In equilibrium it is certainly incorrect to have μ_{As} as high as assumed by Kaxiras *et al.*; (ii) real growth situations are done at pressures for which bulk As does not form. Since by lowering the temperature bulk As can be grown, as is routinely done to form a cap of As on the sample.²⁴ This means that at the higher growth temperature in real situations, μ_{As} is definitely below the bulk value, not 1.15 eV above it; and (iii) if it is argued that one is dealing with a nonequilibrium situation which violates the above equilibrium conditions, then it is also necessary to consider the rates for many competing processes, one of which is still the growth of bulk elemental material.

B. Total energies of bulk GaAs, Ga, and As; heats of formation

It follows from the above analysis that in order to determine the ranges of the chemical potentials, it is necessary to first calculate the total energies of the bulk forms of Ga, As, and GaAs. We are faced with the problem of finding the best procedure for making the theoretical calculations most accurate and meaningful. Should we calculate the bulk energies directly or should we calculate the atomic energies and use experimental cohesive energy data to arrive at the bulk energies? Since the predictions of surface-energy dependence on stoichiometry depend crucially upon the accuracy of these energies (errors of ~ 0.1 eV can change the conclusions), it is important to make the choice which minimizes the errors.

The "standard" states of Ga and As which we choose here are the bulk, solid states. The reason for this is that errors inherent in the local-density approximation (LDA) and errors due to numerical inaccuracies in the calculations cancel best if we consider energy differences between solid phases of similar densities. There is an important test for our results: since we calculate independently the energies for bulk Ga, As, and GaAs, comparison with the measured heat of formation for GaAs is a meaningful test. We discuss this in detail below.

We may note that a different choice of "standard" states was made in Ref. 7. In that work, LDA calculations of energies were made for bulk GaAs and *atomic* Ga and As. Energies of other phases of Ga and As were found using *experimental* values for their energies relative to the atoms. We believe such a procedure has the possibility of introducing significant errors due to the inadequacy of the LDA for atoms. It is well known that the errors are larger for atoms, especially for open-shell atoms like Ga and As, than for nearly-free-electron bulk solids, like GaAs, Ga, or As.²⁵ Although the authors of Ref. 7 have shown that they find the correct cohesive energy for GaAs, our analysis below shows this happens only because of a fortuitous cancellation of the sum of LDA errors for the two atoms and the cutoff error in the bulk calculation for GaAs. For *sp*-bonded material (such as Si, Ge, Mg, Al, GaAs, etc.), the cohesive energies calcu-

lated in LDA are overestimated by ~ 0.6 – 1 eV.²⁶ Since they use experimental cohesive energies for Ga and As, it follows that the heat of formation is also correct in their work. However, even in the case that the sum of errors cancel for the heat of formation, there may yet be errors in the individual energies of bulk Ga and As, i.e., in the limits on the chemical potentials. Any difference in the LDA errors for Ga and As atoms will shift the resulting energies for the elements used in Ref. 7. An analysis of the LDA errors in the atoms could resolve this point.

Our calculations for bulk GaAs have already been described in the previous section. For Ga and As, we have carried out LDA calculations with identical cutoffs and potentials. For each of these elements, there is the complication that the lowest-energy phases have distorted low-symmetry metallic structures.²⁷ Since As has been previously considered in exhaustive detail²⁸ using the same method as in the present work, we need to say here only that we calculated the present energy for the experimental structure using a set of 44 inequivalent k points. The calculated energies are given in Table II.

To our knowledge, there has been no previous fully-self-consistent local-density calculations for Ga. There has been, however, considerable earlier theoretical work²⁹ which we can build upon here. Because the lowest-energy phase of Ga is a complicated orthorhombic structure with eight atoms per cell, we report a full calculation only for a 6-Ry cutoff with the soft potential. For this calculation we used 75 inequivalent k points to sample the primitive Brillouin zone. Using the experimental structure (the values at 4.2 K given in Ref. 27), we found the energy to be -62.082 eV/atom; we then minimized the energy with respect to the volume and the internal parameters y and z , but we kept the ratio of the lattice constants $a:b:c$ fixed. The resulting lattice constant and parameters, compared to the experimental values at 4.2 K given in parentheses, are as follows: $a=4.35$ Å (4.52 Å), $y=0.161$ (0.154), and $z=0.085$ (0.080). The energy is -62.161 eV/atom, which is our predicted lowest ener-

gy of Ga for the soft potential at 6-Ry cutoff, as given in Table II. In order to find the predicted bulk energies for the other cases, we made use of the idea given in Ref. 29 that the energy is similar for Ga in the simple fcc structure. For the soft potential at 6-Ry cutoff we found the minimum energy for the fcc structure to be 0.20 eV/atom higher than for the optimized orthorhombic structure. (Therefore, we conclude that we have verified to this extent that LDA predicts the correct distorted structure of Ga and that we have found an accurate total energy for bulk Ga.) For all other cases we considered only the fcc structure. In each case we found the minimum energy for fcc and we arrived at the predicted energy for orthorhombic Ga by subtracting 0.20 eV/atom. These are the energies for Ga given in Table II.

From the above calculations, we have determined the heat of formation of GaAs from bulk Ga and As. The results are given in Table II, where they are compared with experiment. We see that for an accurate calculation (12-Ry cutoff) and a hard pseudopotential there is essentially exact agreement with experiment. An almost identical heat of formation was also found in a calculation using the pseudopotential generated by Bachelet *et al.*¹³ at an 18-Ry energy cutoff. The agreement with experiment is not unexpected, since the LDA is known to give accurate results for the energy differences in similar cases. For example, LDA calculations have been very successful for energy differences between the semiconducting and high-pressure metallic phases of many semiconductors.^{30,31} We may note that the experimental values are at room temperature whereas the theory is for $T=0$; the agreement argues well for our approximation of ignoring the T dependence of the differences in free energies of different condensed phases.

We also see in Table II that there is an error of ~ 0.35 eV in the heat of formation ΔH_f introduced by our less accurate soft pseudopotential. This, however, is not a serious problem. We can calculate the changes in ΔH_f due to a softening of the Ga and the As potentials sepa-

TABLE II. Total energies of GaAs, Ga, and As and the heat of formation ΔH_f in units of eV/atom for the elements and eV/molecule for GaAs. The pseudopotentials denoted hard and soft are norm-conserving nonlocal potentials described in the text. Results shown in parentheses are calculated with a 6-Ry cutoff on the plane waves; others are with a 12-Ry cutoff. The values in the last row have been corrected as described in the text; the corrected 6-Ry values are used for the surface calculations in the remainder of the paper.

	GaAs	Ga	As	Heat of formation
Measured ^a				0.74
Hard Ga,As ^b	-235.379	-61.364	-173.294	0.72
Hard Ga,As ^c	-235.832	-62.613	-172.490	0.73
	(-230.825)	(-60.988)	(-168.075)	(1.76)
Soft Ga,As ^c	-237.512	-62.364	-174.070	1.08
	(-236.168)	(-62.161)	(-172.823)	(1.18)
Soft Ga,As	-237.512	-62.538	-174.245	0.73
Corrected ^c	(-236.168)	(-62.388)	(-173.051)	(0.73)

^aThe measured heat of formation is from Ref. 23.

^bPotential generated from Ref. 13 at an energy cutoff of 18 Ry.

^cPotential generated from Ref. 12.

rately by carrying out calculations with only one potential softened. From such calculations, we find that the changes in ΔH_f are produced equally (to within 0.01 eV) by the soft Ga potential and the soft As potential. Thus the correction may be made by lowering the energies of the Ga and As reservoirs by $0.35/2=0.175$ eV/atom, while keeping the energy of GaAs fixed. Finally, we also give in parentheses in Table II the results if we use a 6-Ry instead of a 12-Ry cutoff. We see that the large error (~ 1 eV) is introduced for the hard potentials whereas a much smaller change (~ 0.11 eV) occurs for the soft ones. Since in our actual surface calculations we used a 6-Ry cutoff, we correct for the additional small error of 0.11 eV by assuming that this error is also equally distributed between Ga and As. The results of our "corrected" values for the Ga and As energies are displayed in Table II; these can be compared exactly with the surface calculations, since all approximations are the same and systematic errors will cancel. Thus we believe that our final energies for the bulk states, needed for analysis of our surface calculations below, are accurate to within a few hundredths of an eV/atom, including all errors due to the LDA, pseudopotential, and numerical approximations.

IV. STRUCTURES OF Ga- and As-TERMINATED GaAs(100) SURFACES: RESULTS

The GaAs(100) surface calculations were done using a slab geometry with a surface at each side. The translational invariance of the surface is preserved in the two directions parallel to the surface (i.e., x - y directions) while in the z direction we have constructed a superlattice consisting of GaAs slabs separated by vacuum. In order to avoid using unnecessarily large unit cells, we modeled the bottom layer of the slab by fractionally charged Ga atoms which were properly chosen to prevent charge transfer from the top layer. This is similar to what was done for the (111) surface by Kaxiras *et al.*⁷ The arsenic layer above this bottom layer was frozen throughout the calculation. The Ga-terminated surfaces were considered using a five-layer slab plus a three-layer vacuum region, while As-terminated surface was modeled by a six-layer slab plus a two-layer vacuum region (or a four-layer slab plus a four-layer vacuum region for test calculations). We are interested in the top layers of the slab, which may be reconstructed in different ways. Since the superlattices (slab plus vacuum region) have the same thickness, we can use exactly the same points in the surface primitive Brillouin zone in the energy summations so that systematic errors will be minimized when taking energy differences. In the case where the total numbers of atoms are different for two systems under comparison, accurate relative energies can be found as long as we have the accurate energy for the reservoir atoms. This was discussed in detail in the preceding section.

In order to establish the absolute energies of these surfaces, we did one slab calculation without artificially charged Ga-like atoms. This slab was chosen to have the Ga(100)- 1×2 relaxed surface with surface Ga coverage $\Theta = \frac{1}{2}$ at both sides. Thus the numbers of Ga and As atoms are equal, and we can directly calculate the surface

energy, as will be described in IV A. The total energies for other surfaces can be obtained from their energies relative to this surface. The calculated surface energies are shown in Table III. We will discuss these results in Secs. IV A–IV D. Some of our results for the Ga-terminated surface have been reported in a previous paper.⁵

A. Ga-terminated missing row model ($\Theta_{\text{Ga}} = \frac{1}{2}$)

The calculations for this surface with a half-monolayer Ga coverage were done for three cases: (i) the ideal, unrelaxed 1×2 surface; (ii) the fully relaxed 1×2 surface; (iii) a 2×2 vacancy-dimer configuration. Figure 2 shows the top view of the Ga(100) surface of GaAs. Figure 2(a) shows both the ideal and relaxed $\Theta_{\text{Ga}} = \frac{1}{2}$ Ga-terminated (missing Ga row) 1×2 surfaces. Figure 2(b) represents the 2×2 reconstruction of the surface where the remaining Ga atoms dimerize.

The total energy of each configuration was calculated as described at the beginning of this section. The atomic positions for the relaxed and dimerized structures are summarized in Table IV. The charge density contour plots for both cases are shown in Figs. 3 and 4. Two features were worth mentioning: (1) For the relaxed missing Ga row surface, the remaining surface Ga atoms relax inward into the As plane, becoming practically coplanar with the As atoms. There is good agreement between the present calculations and a previous tight-binding calculation.⁴ The bond length between the Ga surface atom and the second-layer As atom is compressed by 8% compared to the ideal bulk distance. The As atoms are pushed away but not far enough to form As—As bonds. (2) For the dimerized surface, the Ga—Ga bond length is 2.45 Å. Both the relaxed and dimerized structures appear to form nonmetallic surfaces with gaps ~ 1 eV. However, we have not investigated the bands in detail.

The determination of the surface energy requires an additional calculation. After the 1×2 surface is completely relaxed, we form a five-layer slab with one-half a monolayer Ga coverage at both sides and no fractionally charged atoms. The two surfaces are the same except for a 90° rotation, so that the periodicity is 2×2 . We calculated the total energy for this system which contains eight Ga and eight As atoms. Since this surface has the same stoichiometry as the bulk, we can calculate the surface energy directly. To do this, we fill the three-layer vacuum region to make bulk GaAs and calculate the total energy with exactly the same energy cutoff and special points in the reciprocal lattice. Subtracting the "bulk" energy for the extra three layers, the surface energy determined from the difference in total energies is given as the "relaxed" energy in the upper central column of Table III. To our knowledge, this is the first time that the surface energy of any reconstructed GaAs(100) surface has been obtained. The energies for other structures in the upper central column of Table III are determined relative to this energy. We notice that the surface energy for relaxed vacancy and dimer-vacancy structures are comparable, the energy being a little lower for the dimer-vacancy structure.

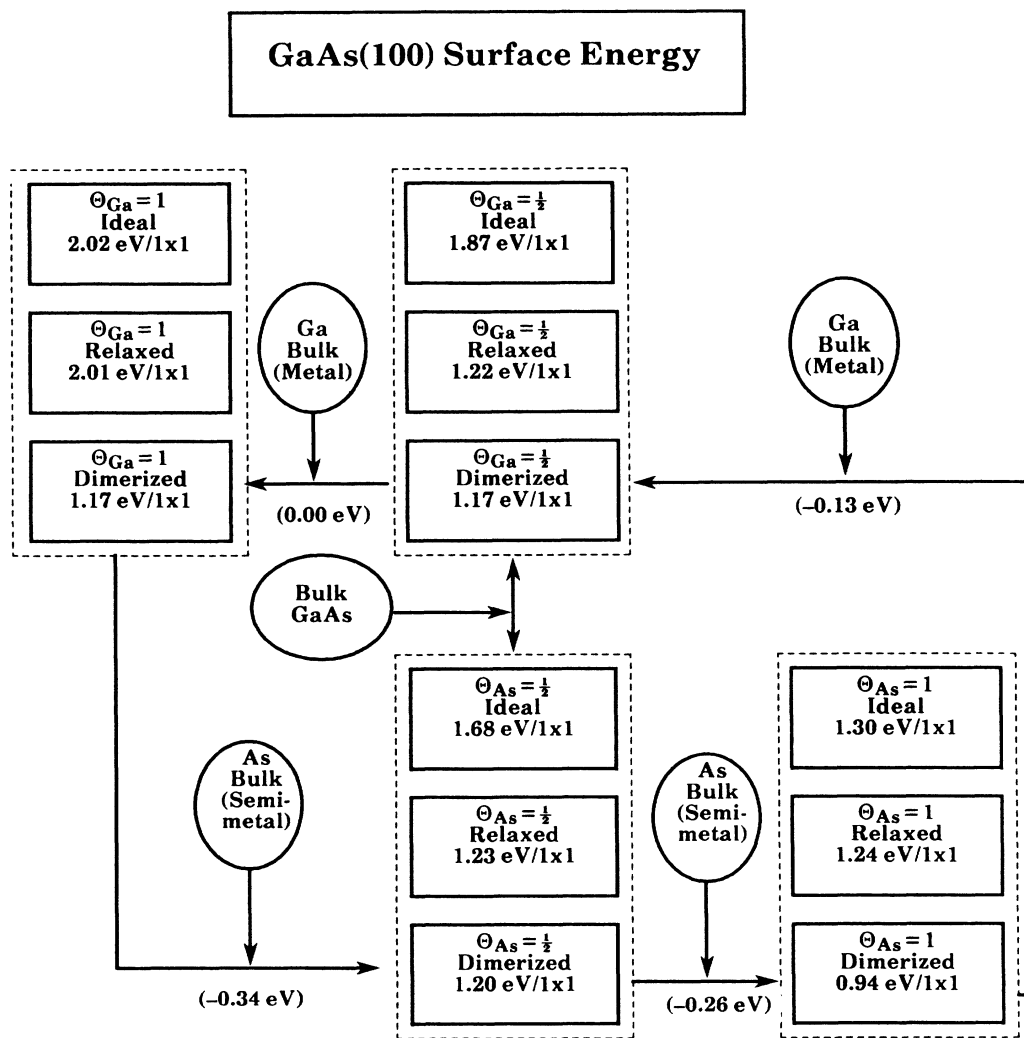
B. Ga-terminated full coverage surface ($\Theta_{\text{Ga}}=1$)

Figures 2(c) and 2(d) show top views of the relaxed 1×1 and dimerized 2×1 Ga-terminated (100) surfaces. The major difference between this surface and the Ga-terminated missing row surface is that here we are dealing with a metallic and polar surface. However, it turns out that using eight sampling points in the surface primitive Brillouin zone for a 2×1 surface is enough to find the total energy by summing states up to the Fermi energy.

The surface energies for ideal, relaxed and dimerized structures are summarized in the upper left column of Table III. Here the surface energy for the dimerized structure is much lower (0.83 eV per 1×1 surface area) than that for the relaxed structure. The relaxation effects

are small because there are no missing surface atoms to allow the Ga atoms to relax inward. The Ga-Ga dimerization reduces the energy by 1.70 eV per dimer compared with the ideal surface. The atomic geometry for this surface is listed in Table V. In order to compare with the surface energy discussed above for the $\Theta_{\text{Ga}}=\frac{1}{2}$ surface, we must consider the chemical potential for adding extra Ga atoms. To do this, we require that the extra Ga atoms come from the most stable state of Ga, a metallic bulk gallium reservoir, as we discussed in Sec. III. As shown in Table III, the surface energy of $\Theta_{\text{Ga}}=1$ is comparable to that of $\Theta_{\text{Ga}}=\frac{1}{2}$. This indicates that the minimum surface energy should occur for a surface Ga coverage of between $\frac{1}{2}$ and 1. Models³² with a coverage of $\frac{3}{4}$ with a 4×2 or $c8 \times 2$ surface periodicity are therefore suggested by the present work.

TABLE III. The surface energy for the GaAs(100) surfaces with different stoichiometries where Θ represents the surface coverage of the element which appears in the subscript. The energies of the stoichiometric $\Theta=\frac{1}{2}$ surfaces are the absolute energies required to create the surface from bulk. For the other surfaces, the energy differences depend on the appropriate reservoir energies. The chosen reservoirs are given in parentheses for each arrow. We also assign total energies to these surfaces with the convention that the energy gained in going from $\Theta_{\text{As}}=1$ ($\Theta_{\text{Ga}}=1$) to $\Theta_{\text{Ga}}=\frac{1}{2}$ ($\Theta_{\text{As}}=\frac{1}{2}$) surfaces is the difference in energies minus $\Delta H_f/2$. Note that the energy gain in a complete cycle is the heat of formation (0.73 eV).



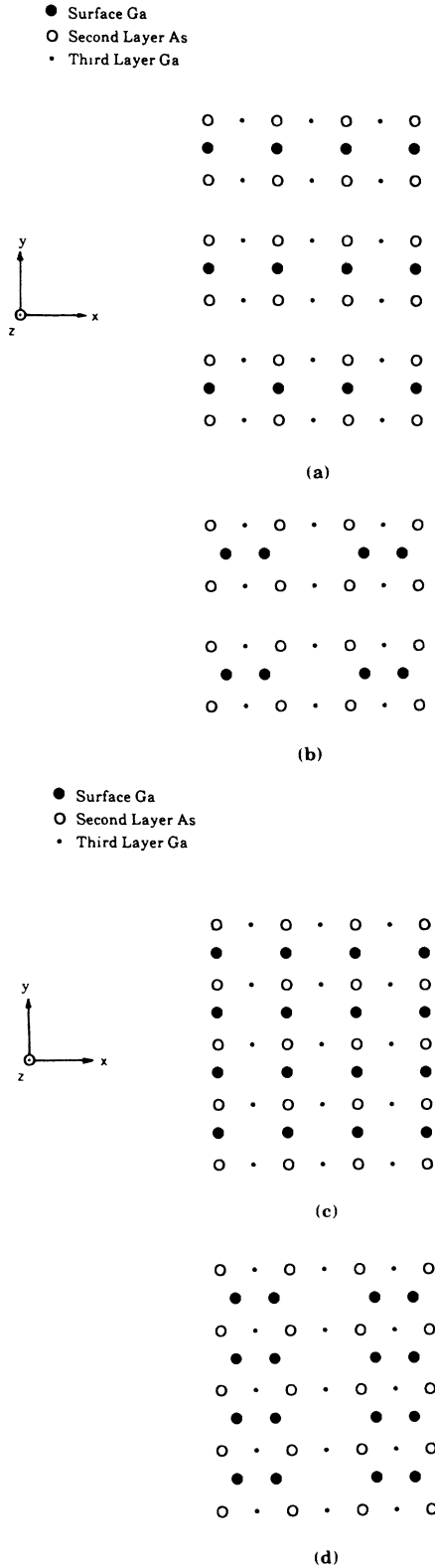


FIG. 2. Top view of the proposed GaAs(100) surface: (a) (1×2) missing row model, $\Theta_{\text{Ga}} = \frac{1}{2}$, representing the ideal and relaxed geometry. The relaxation of this surface results in surface Ga atoms sinking into the second-layer As plane, as shown in Fig. 3. (b) (2×2) vacancy plus dimer model, $\Theta_{\text{Ga}} = \frac{1}{2}$. (c) (1×1) ideal and relaxed geometry, $\Theta_{\text{Ga}} = 1$. (d) (2×1) dimer model, $\Theta_{\text{Ga}} = 1$.

C. As-terminated missing row model ($\Theta_{\text{As}} = \frac{1}{2}$)

For the As vacancy reconstructed surface, we consider three cases similar to that of the Ga vacancy surfaces described in Sec. IV A: (i) the ideal unrelaxed 2×1 surface; (ii) the fully relaxed 2×1 surface; and (iii) a 2×2 vacancy-dimer configuration. As described at the beginning of Sec. III, a six-layer slab geometry plus a two-layer vacuum region was used in these calculations. A calculation with a four-layer slab and a four-layer vacuum region for the ideal unrelaxed 2×1 surface gives a surface energy 0.066 eV per 1×1 surface cell higher than that of an ideal surface of $6 + 2$ layers. This is a measure of the error bar for the calculated surface energies.

Although a simple counting of dangling bonds shows that this surface can be nonmetallic, accidental band crossings make the surface metallic. Each slab has an extra pair of GaAs atoms in comparison to the $\Theta_{\text{Ga}} = \frac{1}{2}$ surface. We can compare the energy of the $\Theta_{\text{As}} = \frac{1}{2}$ surface with that for $\Theta_{\text{Ga}} = \frac{1}{2}$ by subtracting the energy of one GaAs pair. This is equivalent to considering the surface atoms to be in equilibrium with a bulk GaAs reservoir as indicated in Table III. The energies are displayed in the lower center of Table III. The dimerized surface has the lowest surface energy which is a little below that of a relaxed surface, as in the case of the Ga(100) surface. However, for the relaxed surface, the atomic geometry is completely different from that of the Ga(100) surface, as is evident from the charge-density contour plot in Fig. 5. We find that the surface As atoms move out 0.18 Å (13% of the layer separation) towards the vacuum. The second-layer Ga atoms move laterally towards the surface As atoms so that the bond length is reduced to 93% of its bulk value. For the dimerized structure, for which the contour plot is given in Fig. 6, the As atoms move out even more (21% of the layer separation) and the bond length of As-As dimer is found to be 2.63 Å. All the atomic positions for the relaxed and dimerized structures are summarized in Table IV.

D. As-terminated full coverage surface ($\Theta_{\text{As}} = 1$)

For this surface, we have performed similar calculations as described in the preceding section. Top views of the relaxed and dimerized surfaces can be seen in Figs. 2(c) and 2(d) if we interchange Ga and As sites. The slab model is the same as described in Sec. IV C, except that here we do not have missing As rows. The extra As atoms are considered to come from a bulk As reservoir. The surface energies are summarized in the lower right part of Table III, where again we see that dimerized structure substantially reduces the surface energy. Each As-As dimer reduces the energy by 0.7 eV. The As-As bond length is 2.52 Å, which agrees well with 2.55 Å found in the Si(100):As system.¹⁷ The atomic positions can be found in Table V.

We have also considered the asymmetric dimer model³³ for this surface. Starting from the $p2 \times 2$ geometry given in Ref. 33, we found that its surface energy was al-

ways higher than that of the symmetric dimer. Force calculations indicate that asymmetric dimers move to lower their asymmetry and to restore a symmetric configuration. Therefore we find symmetric dimers to be the most stable and we do *not* find the large lowering of energy for the $p2 \times 2$ surface reported in Ref. 33.

Comparing the surface energies of As(100) surface with $\Theta_{As} = \frac{1}{2}$ and $\Theta_{As} = 1$ in Table III, we see that the energy is 0.26 eV per 1×1 surface cell lower for the $\Theta_{As} = 1$ case. Can we conclude from this that in the presence of excess bulk As, a full layer of As on GaAs is more favorable than any fractional coverage? We can definitely say that under this condition, the growth of a full layer of As is more favorable (by 0.26 eV per surface atom) than the missing row model if the surface unit cell is restricted to be 2×2 . However, we have not considered the effects of larger unit cells on the total energy with our *ab initio* method. Tight-binding calculations⁴ for a 2×4 missing row model show it to be approximately 0.3 eV per 1×1 cell lower in energy than for a 2×2 cell. The results are described in the following section.

V. DISCUSSION OF SURFACE ENERGIES

In the previous sections, we have presented our results for the energies of four different types of (100) surfaces of GaAs, with the outermost surface layers having concentrations of $\Theta_{Ga} = 1$ and $\frac{1}{2}$ and $\Theta_{As} = 1$ and $\frac{1}{2}$. In each case, the lowest energy was found for a dimerized structure; however, for the half-filled missing row structures, the relaxed state was at only a slightly higher energy. Furthermore, asymmetries were found for the energies of

adding Ga and As atoms from bulk reservoirs. Here we complement these findings by additional results from our previous work on the (110) surface and from tight-binding calculations,⁴ and we discuss the implications for stability of (100) surfaces under the full range of possible equilibrium conditions.

First, we discuss the relation of the energies of the (110) and (100) surfaces. For the special cases of $\Theta = \frac{1}{2}$, a slab with an odd number of layers can have exactly the *same* structure on its top and bottom surfaces. This means that the slab has an equal number of Ga and As atoms per unit cell and has bulk stoichiometry. The surface energy for $\Theta = \frac{1}{2}$ surfaces can be compared directly, therefore, with that of the (110) surface or with the bulk. The (110) cleavage surface is expected to set a *lower* bound for the energy *per unit area* of the stoichiometric (100) surfaces. Using the ratio of the areas of the cells, this means that the energy per 1×1 cell for the (100) surfaces should be greater than $1/\sqrt{2}$ times the corresponding number of the (110) surface,⁶ i.e., $1.22/\sqrt{2} = 0.86$ eV per cell. In addition, if the energy (per 1×1 cell) exceeds that of the (110) surface, then it is straightforward to show that the (100) surfaces would be unstable to creation of (110) facets. This energy of 1.22 eV per 1×1 cell is therefore a natural *upper* limit on the (100) energy beyond which the nature of the surface would change. This range of surface energies is shown by the vertical line in Fig. 7, for surfaces with equal numbers of Ga and As atoms. We see that our results given in Table III are just barely below the upper limit; the lower limit will be interesting when we discuss (100) surfaces with larger unit cells that have lower energies.

TABLE IV. Surface atomic relaxations and reconstructions for half-monolayer Ga and half-monolayer As-terminated GaAs(100) surface. Refer to Figs. 2(a) and 2(b) for Cartesian coordinate systems. The origin of the coordinates is taken to be the ideal Ga (As) atom position. For the 2×2 dimerized structures, the other surface Ga (As) atom and the second layer As (Ga) atoms are mirror symmetric to the one shown on the table with respect to $x = \sqrt{2}/4$ plane. All numbers in this table are in units of 5.52 Å, the theoretical GaAs lattice constant calculated from the present pseudopotential.

	Ga(100), $\Theta_{Ga} = \frac{1}{2}$			As(100), $\Theta_{As} = \frac{1}{2}$		
	Relaxed	Dimerized		Relaxed	Dimerized	
First layer						
x	0	0 + 0.131		0	0 + 0.115	
y	0	0		0	0	
z	0 - 0.224	0 - 0.187		0 + 0.032	0 + 0.053	
Second layer						
x	0	0 - 0.005		0	0 + 0.013	
y	$\sqrt{2}/4 + 0.044$	$\sqrt{2}/4 + 0.031$		$\sqrt{2}/4 - 0.100$	$\sqrt{2}/4 - 0.093$	
z	$-\frac{1}{4} + 0.027$	$-\frac{1}{4} + 0.013$		$-\frac{1}{4} - 0.032$	$-\frac{1}{4} - 0.013$	
x	0	0 - 0.005		0	0 + 0.013	
y	$-\sqrt{2}/4 - 0.044$	$-\sqrt{2}/4 - 0.031$		$-\sqrt{2}/4 + 0.100$	$-\sqrt{2}/4 + 0.093$	
z	$-\frac{1}{4} + 0.027$	$-\frac{1}{4} + 0.013$		$-\frac{1}{4} - 0.032$	$-\frac{1}{4} - 0.013$	
Third layer						
x	$\sqrt{2}/4$	$\sqrt{2}/4$	$-\sqrt{2}/4$	$\sqrt{2}/4$	$\sqrt{2}/4$	$-\sqrt{2}/4$
y	$\sqrt{2}/4 + 0.0004$	$\sqrt{2}/4 + 0.005$	$\sqrt{2}/4 - 0.0007$	$\sqrt{2}/4 + 0.009$	$\sqrt{2}/4 + 0.011$	$\sqrt{2}/4 - 0.004$
z	$-\frac{1}{2} + 0.023$	$-\frac{1}{2} + 0.031$	$-\frac{1}{2} + 0.012$	$-\frac{1}{2} + 0.011$	$-\frac{1}{2} + 0.008$	$-\frac{1}{2} + 0.032$
x	$\sqrt{2}/4$	$\sqrt{2}/4$	$-\sqrt{2}/4$	$\sqrt{2}/4$	$\sqrt{2}/4$	$-\sqrt{2}/4$
y	$-\sqrt{2}/4 - 0.0004$	$-\sqrt{2}/4 - 0.005$	$-\sqrt{2}/4 + 0.0007$	$-\sqrt{2}/4 - 0.009$	$-\sqrt{2}/4 - 0.011$	$-\sqrt{2}/4 + 0.004$
z	$-\frac{1}{2} + 0.023$	$-\frac{1}{2} + 0.031$	$-\frac{1}{2} + 0.012$	$-\frac{1}{2} + 0.011$	$-\frac{1}{2} + 0.008$	$-\frac{1}{2} + 0.032$

We have pointed out in Sec. III that the stability of surfaces allowing variations in the numbers of Ga and As atoms, depends upon the chemical potentials of Ga and As. The function to be minimized is the energy for variable stoichiometry given in Eq. (2), in which the chemical potentials enter simply as coefficients of terms linear in the number of each type of atom. If we define

$$n_{\text{tot}} = n_{\text{As}} + n_{\text{Ga}} \quad (3a)$$

and

$$\Delta n = n_{\text{As}} - n_{\text{Ga}}, \quad (3b)$$

then the energy in Eq. (2) may be written

$$E - (\mu_{\text{Ga}} n_{\text{Ga}} + \mu_{\text{As}} n_{\text{As}}) = E - \frac{1}{2}(\mu_{\text{Ga}} + \mu_{\text{As}}) n_{\text{tot}} + \frac{1}{2}(\mu_{\text{Ga}} - \mu_{\text{As}}) \Delta n. \quad (4)$$

Although the sum of chemical potentials is fixed by equilibrium with the bulk [Eq. (1a)], the last term may be changed by the experimental conditions. The range of the difference in chemical potentials is easily derived from Eqs. (1a)–(1c) to be

$$-\Delta H_f \leq (\mu_{\text{As}} - \mu_{\text{Ga}}) - (\mu_{\text{As}(\text{bulk})} - \mu_{\text{Ga}(\text{bulk})}) \leq \Delta H_f. \quad (5)$$

The extreme cases which we have considered before cor-

respond to an “As-rich environment” (upper limit on $\mu_{\text{As}} - \mu_{\text{Ga}}$) or a “Ga-rich environment” (lower limit). All other cases have an intermediate coefficient of $\Delta n = (n_{\text{As}} - n_{\text{Ga}})$ in Eq. (4). In Fig. 7 we show the allowable range of the energies for the filled As and Ga surfaces which we have calculated in the previous sections. Although we have not calculated energies for any surfaces with intermediate occupations, we have also drawn in Fig. 7 parabolas fitted to the calculated points which could represent possible other surfaces. We will say more about such surfaces below. Thus the shaded areas in Fig. 7 are meant to represent the family of curves that can be generated by changing the chemical potentials while maintaining equilibrium.

One interesting point can be made by examining the energy change resulting from the exchange of an atom with a bulk reservoir as a function of coverage as shown in Fig. 7(a). The energy gained per atom in going from a filled surface to half-filled [e.g., adding Ga to an As-terminated surface ($\Theta_{\text{Ga}} = 0$) or As to a Ga-terminated surface ($\Theta_{\text{As}} = 0$)] is more than in going from half-filled to filled (e.g., adding Ga to go from $\Theta_{\text{Ga}} = \frac{1}{2}$ to $\Theta_{\text{Ga}} = 1$, etc.). That is, there is a net repulsive energy as atoms are added. This is not surprising since we have seen that relaxa-

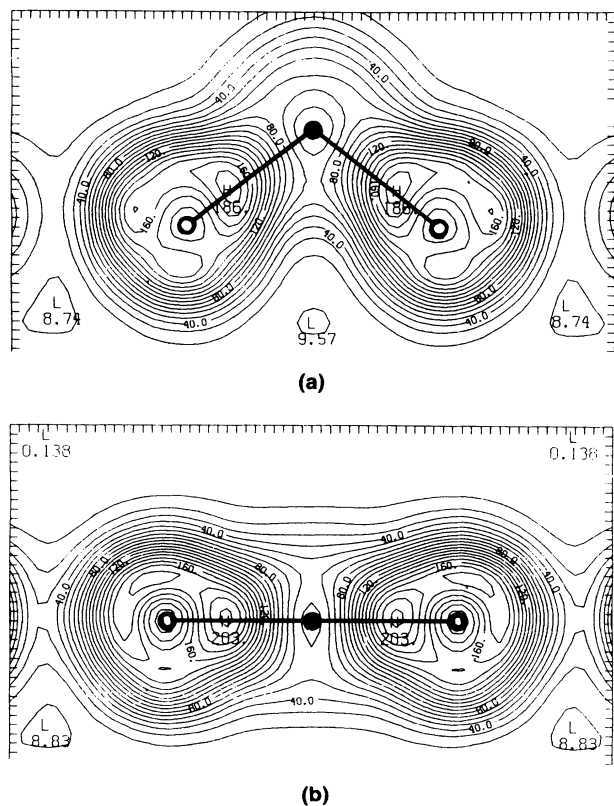


FIG. 3. Charge-density contour plots for the $\Theta_{\text{Ga}} = \frac{1}{2}$ Ga-terminated (100) surface: (a) ideal surface; (b) relaxed surface. It is plotted in the $x = 0$ plane in Fig. 2(a). The Ga atoms are represented by closed circles and the As atoms by open circles. Units are electron/supercell; the volume of our supercells is 336.4 \AA^3 .

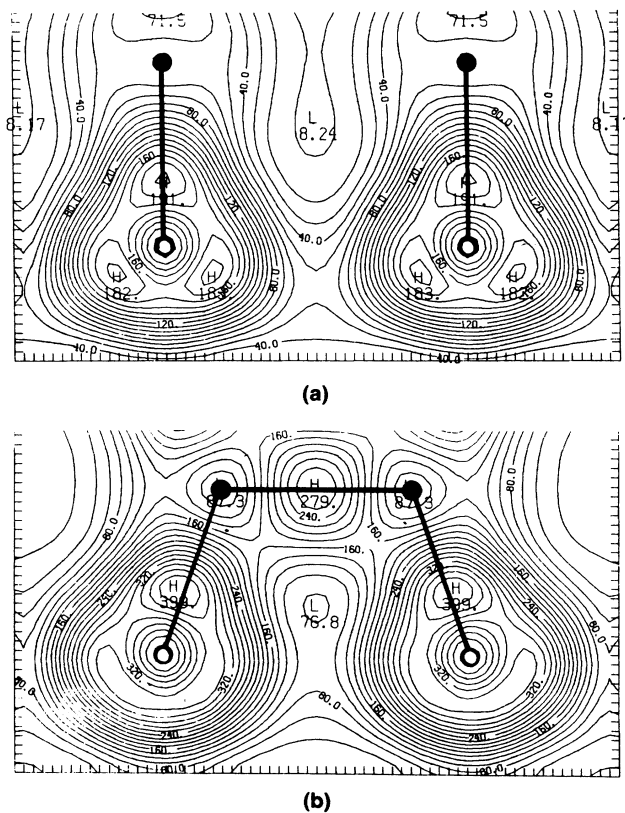


FIG. 4. Charge-density contour plots for the $\Theta_{\text{Ga}} = \frac{1}{2}$ Ga-terminated (100) surface: (a) ideal and (b) with a Ga-Ga dimer. It is plotted in the plane which contains two surface Ga atoms and two second-layer As atoms. The Ga atoms are represented by closed circles and the As atoms by open circles. Units are electron/supercell; the volume of our supercells is 336.4 \AA^3 for (a) and 672.8 \AA^3 for (b).

TABLE V. Surface atomic relaxations for full Ga (As) surface coverage GaAs(100) surface. Refer to Figs. 2(c) and 2(d) for Cartesian coordinate system. The origin of the coordinates is taken to be the ideal position of a surface Ga (As) atom. All numbers in this table are in units of 5.52 \AA , the theoretical GaAs lattice constant calculated from the present pseudopotential.

		Ga(100), $\Theta_{\text{Ga}}=1$		As(100), $\Theta_{\text{As}}=1$		
		Relaxed	Dimerized	Relaxed	Dimerized	
First layer						
x	0		$0 + 0.144$	0	$0 + 0.126$	
y	0		0	0	0	
z	$0 - 0.028$		$0 - 0.073$	$0 - 0.006$	$0 + 0.019$	
Second layer						
x	0		$0 - 0.016$	0	$0 + 0.028$	
y	$\sqrt{2}/4$		$\sqrt{2}/4$	$\sqrt{2}/4$	$\sqrt{2}/4$	
z	$-\frac{1}{4} + 0.016$		$-\frac{1}{4} + 0.022$	$-\frac{1}{4} + 0.014$	$-\frac{1}{4} + 0.036$	
Third layer						
x	$\sqrt{2}/4$	$\sqrt{2}/4$	$-\sqrt{2}/4$	$\sqrt{2}/4$	$\sqrt{2}/4$	$-\sqrt{2}/4$
y	$\sqrt{2}/4$	$\sqrt{2}/4$	$\sqrt{2}/4$	$\sqrt{2}/4$	$\sqrt{2}/4$	$\sqrt{2}/4$
z	$-\frac{1}{2} + 0.009$	$-\frac{1}{2} + 0.017$	$-\frac{1}{2} - 0.001$	$-\frac{1}{2} + 0.006$	$-\frac{1}{2} - 0.009$	$-\frac{1}{2} + 0.052$

tion is effective in lowering the energy of the partially filled surfaces. In fact, for very low coverages ($\Theta \ll \frac{1}{2}$), the atoms may be in their lowest energy state by relaxing individually instead of dimerizing into pairs. The important point is that the curves representing $E - \sum_i \mu_i n_i$ in Fig. 7(a) have concave curvature. This is essential for the

states at fractional coverage to be stable relative to phase separation into two regions that are more Ga-rich and more As-rich, respectively. When we discuss other more complicated reconstructions below, we will see that surfaces with fractional coverage are further stabilized.

For the Ga-terminated surfaces, we find the result that,

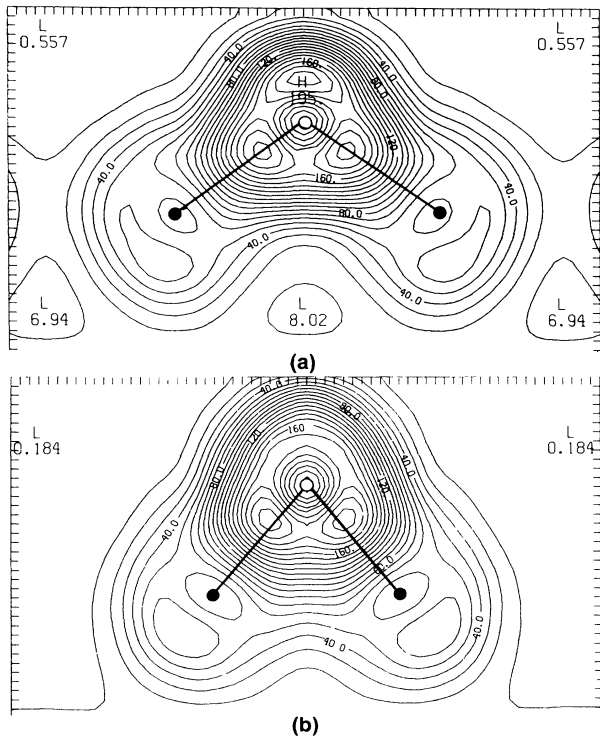


FIG. 5. Charge-density contour plots for the $\Theta_{\text{As}}=\frac{1}{2}$ As-terminated (100) surface: (a) ideal and (b) relaxed surface. It is plotted in the $x=0$ plane in Fig. 2(a) if Ga and As atoms change sites. The Ga atoms are represented by closed circles and the As atoms by open circles. Units are electron/supercell; the volume of our supercells is 336.4 \AA^3 for both (a) and (b).

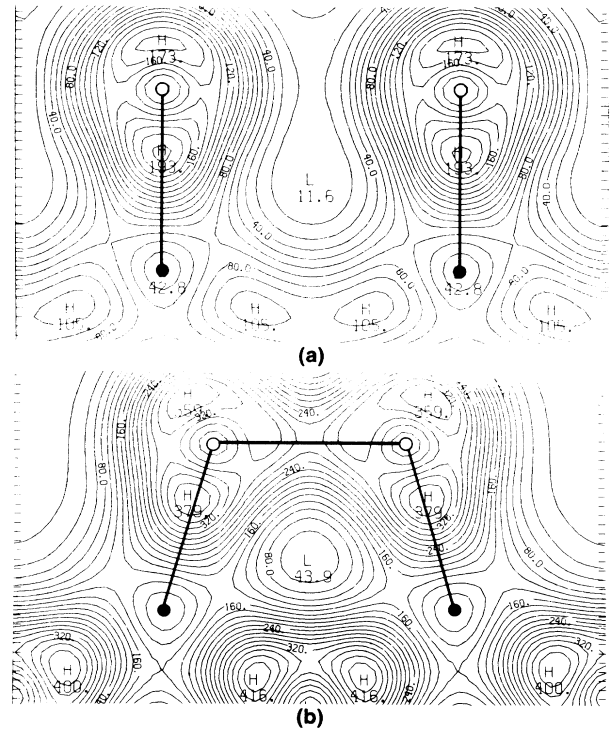


FIG. 6. Charge-density contour plots for the $\Theta_{\text{As}}=1$ As-terminated (100) surface: (a) ideal and (b) with a As-As dimer. It is plotted in the plane which contains two surface As atoms and two second-layer Ga atoms. The Ga atoms are represented by closed circles and the As atoms by open circles. Units are electron/supercell; the volume of our supercells is 336.4 \AA^3 for (a) and 672.8 \AA^3 for (b).

within the restrictions of a 2×2 periodicity, the energies are essentially identical for $\Theta_{\text{Ga}} = \frac{1}{2}$ and $\Theta_{\text{Ga}} = 1$ coverage when the surface is in equilibrium with bulk Ga. This means that the partially filled surface is just as stable as the filled surface, even in equilibrium with excess Ga in the bulk metallic state. Tight-binding calculations indicate, however, that there is an extra stabilization energy for the half-monolayer coverage case when the unit cell is enlarged to 2×4 . The stabilization does not arise from a better relaxation energy but comes from orbital rehybridizations which are possible in a 2×4 geometry but not in a 2×2 one. These results suggest, therefore, that it is likely that the minimum energy structure will occur for $\frac{1}{2} < \Theta_{\text{Ga}} < 1$. A coverage of $\frac{3}{4}$ has been suggested by re-

cent experimental work on annealed GaAs, in a Ga-rich environment.³²

For the As-terminated $\Theta_{\text{As}} = \frac{1}{2}$ surface, the energy is reduced when As atoms are taken from a bulk As reservoir and placed on the surface. If one assumes the atoms are taken from an As_2 reservoir, then the energy is lowered by an extra 1.15 eV/atom. However, we have argued in Sec. III that it is not appropriate to use the molecular reservoir unless one considers the *free energy* of the gas. Our results predict that the fully covered As surface should be reached under conditions of excess As. An important consideration, however, is whether there exist other structures with lower energy than those we have considered here. In particular, both experiments and theory suggest that there are additional reconstructions which need to be considered. These may be grouped into two classes. First, for the fully covered surfaces, we expect that the present 2×1 metallic state is unstable and there will be further reconstructions which will open gaps at the Fermi energy.

Fractional surface coverages involving larger unit cells were examined with the tight-binding method. For the $\Theta_{\text{As}} = \frac{1}{2}$ surface, the vacancy-dimer model was examined with both a 2×2 (the same as discussed above) and a 2×4 cell. The lowest energy was found for pairs of dimer rows separated by pairs of missing rows where the rows are defined to be aligned along the dimerization axis of the surface As atoms.⁴ The calculated 2×4 surface energy is substantially (0.30 eV per 1×1 cell) below that of the 2×2 cell. The energy reduction arises primarily from a rehybridization of second-layer Ga dangling-bond orbitals which is possible in the 2×4 but not in the 2×2 cell. We have included this energy in our Fig. 7(b) by using the energy difference from our *ab initio* 2×2 calculation. We see that the energy reduction from using the larger 2×4 cell is sufficiently large to make the $\Theta_{\text{As}} = \frac{1}{2}$ surface more stable than the filled surface, even in equilibrium with excess bulk As or excess Ga. It is interesting to note that the energy for this $\Theta = \frac{1}{2}$ surface is just barely above the lower limit in Fig. 7(b), set by the (110) cleavage surface.

We must also consider surfaces with other numbers of Ga and As atoms. Tight-binding calculations were also done⁴ for 2×4 structures with $\Theta_{\text{As}} = \frac{3}{4}$. Since the energy was determined relative to the $\Theta_{\text{As}} = \frac{1}{2}$ vacancy-dimer structures we can place it on the graph in the same relation as to our *ab initio* energy for $\Theta_{\text{As}} = \frac{1}{2}$. Modifying the energy given in Ref. 4 to account for a bulk As reservoir instead of an As_2 reservoir we find the point shown on Fig. 7(b). The surface energy is slightly above the linear interpolation between $\Theta_{\text{As}} = \frac{1}{2}$ and $\Theta_{\text{As}} = 1$. Since the energy differences are small, we conclude that there may be a number of structures with similar energies with $\frac{1}{2} < \Theta_{\text{As}} < 1$ which may be stable as a function of the chemical potential. This appears to be consistent with experimental findings on 2×4 As-rich surfaces. The minimum of the total energy is expected, however, to occur for $\Theta_{\text{As}} > \frac{1}{2}$ because a $\frac{1}{2}$ -monolayer coverage gives rise to *twofold* coordinated Ga atoms in a 2×4 cell.⁴

In Fig. 7 we have drawn parabolic curves passing

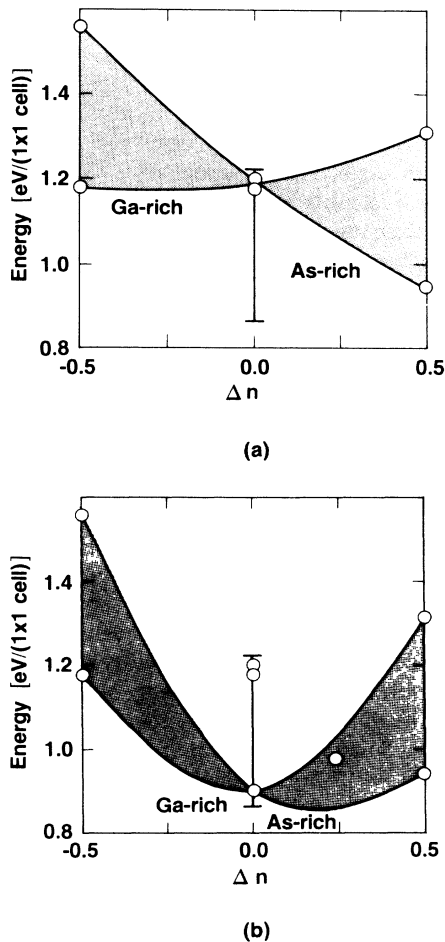


FIG. 7. Energy $E_{\text{surface}}(n_i) - \sum_i \mu_i n_i$ per surface atom as a function of $\Delta n = (n_{\text{As}} - n_{\text{Ga}})$. Part (a) gives the density-functional and (b) density-functional plus tight-binding results. The points are calculated values from Table III for the limiting cases of Ga-rich and As-rich chemical potentials. The curves are parabolas fit through the points as a suggestion of the energies of possible other structures with different stoichiometries. The shaded areas represent the continuous family of curves for intermediate chemical potentials. The minima in (b) suggest the most stable surfaces will be intermediate between half and full coverage.

through the calculated points for the half-filled ($\Delta n = 0$) and filled ($\Delta n = -\frac{1}{2}$ and $\frac{1}{2}$) surfaces. [In Fig. 7(a) we have ignored the small energy difference in the two energies for $\Delta n = 0$.] These represent other possible surfaces with different stoichiometries. The general form can be understood since, in the mean-field approximation, the above-mentioned repulsive interaction between dimers leads to a parabolic form. Of course, there may be energies favoring commensurate structures with simple rational stoichiometries, so that the parabola may be thought of as an approximate envelope for the energies at these special stoichiometries. As a function of the chemical potentials the curves for energy versus Δn can vary between the limiting curves shown in the figures, which are labeled "Ga-rich" and "As-rich"; i.e., there is a family of curves that fills the shaded areas. As shown in Fig. 7(b), the effect of lowering the energy of the surfaces with filling stoichiometry near $\Delta n = 0$ is to reduce the range of variation of the stoichiometries as a function of the chemical potentials. The present results suggest the maximum range may be rather small and that there is a bias toward more As than Ga on the surface.

We close this section by noting that our conclusions concerning the most stable surfaces in the presence of excess Ga or As have depended crucially upon the exact energies of the Ga and As reservoirs. Although we have argued that our LDA calculations are sufficiently accurate for our conclusions, there may yet be errors in these delicate energy differences. On the other hand, these energies do not affect other conclusions, such as the comparison of the energies of dimerization versus relaxation, the surface energy relative to the (110) surface, and the result that $\Theta = \frac{1}{2}$ covered surfaces are more stable than phase-separated regions at $\Theta = 0$ and $\Theta = 1$.

VI. SUMMARY

We have performed *ab initio* calculations on the surface energy and atomic structure of Ga- and As-rich 2×1 , 1×2 , and 2×2 reconstructed GaAs(100) surfaces consisting of various combinations of dimers and vacancies. The local density-functional formalism and soft norm-conserving nonlocal pseudopotentials were used. Equilibrium atomic geometries were determined through minimizations of the total energy. For each surface we

find that the most stable configuration occurs when surface Ga(As) atoms dimerize. Each Ga (As) dimer reduces the energy by 1.7 eV (0.7 eV) from the ideal unrelaxed geometry. The surface energies for $\Theta_{\text{Ga}} = \frac{1}{2}$ and $\theta_{\text{Ga}} = 1$ are found to be comparable (1.17 eV per surface atom) indicating the possibility of a minimum at some intermediate coverage. For the As-terminated surface we find that asymmetric dimers are higher in energy than symmetric dimers. Tight-binding calculations⁴ with symmetric As dimers were done on 2×2 and 2×4 unit cells to determine the effects of unit-cell dimensions on energy and atomic structure. A 2×4 cell is found to lower the energy by 0.3 eV per 1×1 cell as compared to a 2×2 cell. This results from a rehybridization of Ga dangling-bond orbitals in the 2×4 structure which cannot occur within a 2×2 cell. The combination of the *ab initio* and tight-binding calculations suggests that the total energy should be optimal for an As coverage in the range $0.5 < \Theta_{\text{As}} < 1$. Since for $\Theta_{\text{As}} = \frac{1}{2}$ the 2×4 cell gives rise to *twofold* coordinated Ga atoms,⁴ it is expected that the minimum of the total energy will occur at a higher coverage of As than 0.5 monolayers. The tight-binding calculations⁴ indicate that the experimentally observed 2×4 periodicity arises from a surface As coverage of 0.75 monolayer with the As atoms forming an ordered array of dimers separated every fourth row by missing dimers. The recent scanning tunneling microscopy studies of GaAs(100)- 2×4 surfaces by Pashley *et al.*³⁴ provide strong support for this missing row dimer model.

ACKNOWLEDGMENTS

The authors wish to thank C. Van de Walle for much help during the initial stages of our calculations, and S. Froyen for providing us with the computer programs for the atomic calculations. We thank R. Bringans, F. Ponce, Conyers Herring, D. Fenner, and S. Satpathy for useful discussions. We are also indebted to K. Kunc, O. H. Nielsen, and R. J. Needs whose developments we have used. This work is supported in part by the U.S. Office of Naval Research through Contract No. N00014-82-C-0244 and the Division of Materials Sciences, Office of Basic Energy Sciences, U.S. Department of Energy under Contract DE-AC02-76CH00016.

¹J. R. Arthur, *Surf. Sci.* **43**, 449 (1974); A. Y. Cho, *J. Appl. Phys.* **47**, 2841 (1976).

²P. K. Larsen, J. H. Neave, and B. A. Joyce, *J. Phys. C* **14**, 167 (1981).

³R. Z. Bachrach, *Progress in Crystal Growth and Characterization* (Pergamon, London, 1979), Vol. 2, pp. 115–144.

⁴D. J. Chadi, *J. Vac. Sci. Technol. A* **5**, 834 (1987).

⁵Guo-Xin Qian, R. M. Martin, and D. J. Chadi, *J. Vac. Sci. Technol. B* **5**, 933 (1987).

⁶Guo-Xin Qian, R. M. Martin, and D. J. Chadi, *Phys. Rev. B* **37**, 1303 (1988) and references therein.

⁷E. Kaxiras, Y. Bar-Yam, J. D. Joannopoulos, and K. C. Pan-

dey, *Phys. Rev. B* **33**, 4406 (1986); *Phys. Rev. Lett.* **57**, 106 (1986); *Phys. Rev. B* **35**, 9625 (1987); **35**, 9636 (1987); E. Kaxiras, K. C. Pandey, Y. Bar-Yam, and J. D. Joannopoulos, *Phys. Rev. Lett.* **56**, 2819 (1986).

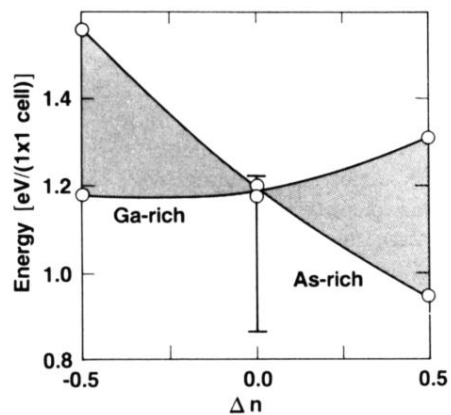
⁸P. Hohenberg and W. Kohn, *Phys. Rev.* **136**, B864 (1964); W. Kohn and L. J. Sham, *Phys. Rev.* **140**, A1133 (1965).

⁹O. H. Nielsen and R. M. Martin, *Phys. Rev. B* **32**, 3792 (1985).

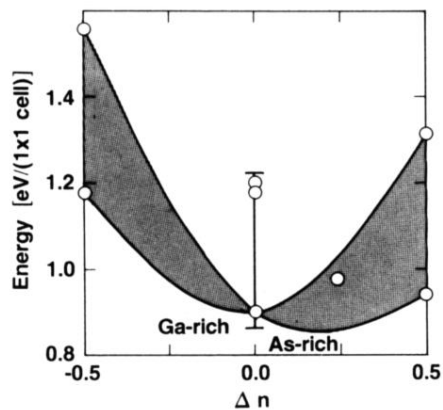
¹⁰O. H. Nielsen, R. M. Martin, D. J. Chadi, and K. Kunc, *J. Vac. Sci. Technol. B* **1**, 714 (1983).

¹¹D. M. Ceperley and B. J. Alder, *Phys. Rev. Lett.* **45**, 566 (1980); J. P. Perdew and A. Zunger, *Phys. Rev. B* **23**, 5048 (1981).

- ¹²G. P. Kerker, *J. Phys. C* **13**, L189 (1980).
- ¹³G. B. Bachelet, D. R. Hamann, and M. Schlüter, *Phys. Rev. B* **26**, 4199 (1982).
- ¹⁴J. E. Northrup, *Phys. Rev. Lett.* **54**, 815 (1985).
- ¹⁵J. E. Northrup and M. L. Cohen, *J. Vac. Sci. Technol.* **21**, 333 (1982); *Phys. Rev. Lett.* **49**, 1349 (1982); K. C. Pandey, *Phys. Rev. Lett.* **49**, 223 (1982).
- ¹⁶S. Froyen and M. L. Cohen, *Phys. Rev. B* **28**, 3258 (1983).
- ¹⁷R. I. G. Uhrberg, R. D. Bringans, M. A. Olmstead, R. Z. Bachrach, and J. E. Northrup, *Phys. Rev. B* **35**, 3945 (1987).
- ¹⁸An extensive list of earlier references for the (110) surface is given in Ref. 6.
- ¹⁹C. Messmer and J. C. Bilello, *J. Appl. Phys.* **52**, 4623 (1981).
- ²⁰T.-C. Chiang, J. A. Knapp, M. Aono, and D. E. Eastman, *Phys. Rev. B* **21**, 3513 (1980); W. Ranke, *Phys. Rev. B* **27**, 7807 (1983).
- ²¹F. Reif, *Fundamentals of Statistical and Thermal Physics* (McGraw-Hill, New York, 1965).
- ²²J. M. Moison, C. Guille, and M. Bensoussan, *Phys. Rev. Lett.* **58**, 2555 (1987).
- ²³*Large's Handbook of Chemistry*, 12th ed., edited by J. A. Dean (McGraw-Hill, New York, 1979), pp. 9–23 and 9-8; *Handbook of Chemistry and Physics*, 65th ed., edited by R. C. Weast (CRC, Boca Raton, 1984), pp. D-53 and D-68.
- ²⁴R. Bringans (private communication).
- ²⁵R. O. Jones, *Phys. Rev. Lett.* **52**, 2002 (1984) and Ref. 5 therein; O. Gunnarsson and R. O. Jones, *Phys. Rev. B* **31**, 7588 (1985); R. O. Jones and O. Gunnarsson, *Phys. Rev. Lett.* **55**, 107 (1985).
- ²⁶M. S. Hybertsen and S. G. Louie, *Phys. Rev. B* **30**, 5777 (1984).
- ²⁷J. Donohue, *The Structures of the Elements* (Krieger, Marabar, FL, 1982).
- ²⁸R. J. Needs, R. M. Martin, and O. H. Nielsen, *Phys. Rev. B* **33**, 3778 (1986); *Phys. Rev. B* (to be published).
- ²⁹V. Heine and D. Weaire, in *Solid State Physics*, edited by H. Ehrenreich, F. Seitz, and D. Turnbull (Academic, New York, 1970), Vol. 24.
- ³⁰R. M. Martin, *Festkörperprobleme*, Vol. 23 of *Advances in Solid State Physics*, edited by P. Grosse (Vieweg, Braunschweig, 1985).
- ³¹M. L. Cohen, *Phys. Scr.* **T1**, 5 (1985).
- ³²D. J. Frankel, C. Yu, J. P. Harbison, and H. H. Farrell, *J. Vac. Sci. Technol. B* **5**, 1113 (1987).
- ³³J. Ihm, D. J. Chadi, and J. D. Joannopoulos, *Phys. Rev. B* **27**, 5119 (1983).
- ³⁴M. D. Pashley, K. W. Haberern, W. Friday, J. M. Woodall, and P. D. Kirchner, *Phys. Rev. Lett.* **60**, 2176 (1988).



(a)



(b)

FIG. 7. Energy $E_{\text{surface}}(n_i) - \sum_i \mu_i n_i$ per surface atom as a function of $\Delta n = (n_{\text{As}} - n_{\text{Ga}})$. Part (a) gives the density-functional and (b) density-functional plus tight-binding results. The points are calculated values from Table III for the limiting cases of Ga-rich and As-rich chemical potentials. The curves are parabolas fit through the points as a suggestion of the energies of possible other structures with different stoichiometries. The shaded areas represent the continuous family of curves for intermediate chemical potentials. The minima in (b) suggest the most stable surfaces will be intermediate between half and full coverage.